THE JOURNAL OF BIOLOGICAL CHEMISTRY Vol. 276, No. 12, Issue of March 23, pp. 9108–9114, 2001
Printed in U.S.A.

Induction of Activator Protein-1 through Reactive Oxygen Species by Crystalline Silica in JB6 Cells*

Received for publication, August 22, 2000, and in revised form, November 2, 2000
Published, JBC Papers in Press, November 28, 2000, DOI 10.1074/jbc.M007666200

Min Ding, Xianglin Shi, YongJu Lu, Chuanshu Huang, Stephen Leonard, Jenny Roberts, Jim Antonini, Vince Castranova, and Val Vallyathan‡

From the Pathology and Physiology Research Branch, Health Effects Laboratory Division, National Institute for Occupational Safety and Health, Morgantown, West Virginia 26505

We reported previously that freshly fractured silica (FFSi) induces activator protein-1 (AP-1) activation through extracellular signal-regulated protein kinases (ERKs) and p38 kinase pathways. In the present study, the biologic activities of FFSi and aged silica (ASi) were compared by measuring their effects on the AP-1 activation and phosphorylation of ERKs and p38 kinase. The roles of reactive oxygen species (ROS) in this silica-induced AP-1 activation were also investigated. We found that FFSi-induced AP-1 activation was four times higher than that of ASi in JB6 cells. FFSi also caused greater phosphorylation of ERKs and p38 kinase than ASi. FFSi generated more ROS than ASi when incubated with the cells as measured by electron spin resonance (ESR). Studies using ROS-sensitive dyes and oxygen consumption support the conclusion that ROS are generated by silica-treated cells. *N*-Acetylcysteine (an antioxidant) and polyvinyl pyridine-*N*-oxide (an agent that binds to Si-OH groups on silica surfaces) decreased AP-1 activation and phosphorylation of ERKs and p38 kinase. Catalase inhibited phosphorylation of ERKs and p38 kinase, as well as AP-1 activation induced by FFSi, suggesting the involvement of H_2O_2 in the mechanism of silica-induced AP-1 activation. Sodium formate (an ·OH scavenger) had no influence on silica-induced MAPKs or AP-1 activation. Superoxide dismutase enhanced both AP-1 and MAPKs activation, indicating that H_2O_2, but not $O_2^{\cdot-}$, may play a critical role in silica-induced AP-1 activation. These studies indicate that freshly ground silica is more biologically active than aged silica and that ROS, in particular H_2O_2, play a significant role in silica-induced AP-1 activation.

Epidemiological and pathologic studies have established that occupational exposure to crystalline silica is associated with the development of pulmonary silicosis (1, 2) and an increased risk for lung cancer (2–4). Silica, administered by inhalation or intratracheal instillation, has been shown to be carcinogenic in rats (4–7). Intrapleural administration of crystalline silica in rats leads to the induction of localized malignant histiocytic lymphomas (8). The pulmonary response to silica, however, was found to vary considerably in different species, with mice developing silicosis but no lung cancer and hamsters just showing storage of silica in lung macrophages with no apparent pathology (4–6). Human evidence is also controversial regarding the induction of lung cancer in workers exposed to silica (3). However, based on evidence obtained from studies with laboratory animals and epidemiological studies in humans, the International Agency for Research on Cancer has classified crystalline silica as a class 1 human carcinogen (9).

Although crystalline silica is a documented carcinogen, the molecular mechanisms involved in the silica-induced carcinogenesis are unclear. Previous studies have shown that silica causes direct DNA damage and mammalian cell transformation (10, 11). Earlier studies have also demonstrated that FFSi[1] is capable of generating hydroxyl radicals (·OH) upon reaction with aqueous media (12–14). Superoxide anion radicals ($O_2^{\cdot-}$) may also be generated (15). The silicon-based free radicals (Si·, SiO·, and SiOO·) and the associated generation of H_2O_2 and ·OH appear to be involved in the lipid peroxidation and membrane damage (12–15). These radicals are also associated with silica-induced DNA damage, for example both strand breakage and hydroxylation of dG residues have been observed (10, 17). $O_2^{\cdot-}$, H_2O_2, and ·OH are generally called reactive oxygen species (ROS). For direct ROS generation via a reaction between silica and aqueous medium in the absence of cells, a relatively large amount of silica particles is needed to generate detectable amounts of ROS. However, silica also can generate ROS via stimulation of cells. In this mechanism of ROS generation, silica induces ROS production as part of the respiratory burst reaction to particles. ROS generated by this mechanism may be responsible for silica-induced activation of the nuclear transcription factor NF-κB (16). However, the mechanism by which ROS from cells stimulated by silica activates AP-1 remains to be investigated fully.

Previous studies from our laboratory showed that FFSi causes AP-1 activation both *in vitro* using cell culture systems and *in vivo* using transgenic mice (18). AP-1 is a transcription factor that consists of either a Jun-Jun homodimer or a Jun-Fos heterodimer (19). Genes regulated by AP-1 have been reported to play an important role in neoplastic transformation, tumor progression, and metastasis (18–22). Blocking 12-*O*-tetradecanolyphorbol-13-acetate-induced AP-1 activation has

* The costs of publication of this article were defrayed in part by the payment of page charges. This article must therefore be hereby marked "*advertisement*" in accordance with 18 U.S.C. Section 1734 solely to indicate this fact.

‡ To whom correspondence should be addressed: Pathology and Physiology Research Branch, National Institute for Occupational Safety and Health, 1095 Willowdale Rd., Morgantown, WV 26505. Tel.: 304-285-5770; Fax: 304-385-5938; E-mail: vav1@cdc.gov.

[1] The abbreviations used are: FFSi, freshly fractured silica; ASi, aged silica; AP-1, activator protein 1; MAPK, mitogen-activated protein kinase; ROS, reactive oxygen species; ESR, electron spin resonance; PVPNO, polyvinyl pyridine-*N*-oxide; ·OH, hydroxyl radical; $O_2^{\cdot-}$ superoxide anion radical; H_2O_2, hydrogen peroxide; SOD, superoxide dismutase; ERK, extracellular signal-regulated protein kinase; *N*-acetyl-L-cysteine; DMPO, 5,5-dimethyl-1-pyrroline-*N*-oxideNAC; MEM, Eagle's minimum essential medium; FBS, fetal bovine serum; K_3CrO_8, potassium tetraperoxochromate; H_2DCFDA, 2′,7′-dichlorodihydrofluorescein diacetate; JNK, c-Jun N-terminal kinase; PBS, phosphate-buffered saline; ANOVA, analysis of variance; G, Gauss.

This paper is available on line at http://www.jbc.org

Downloaded from http://www.jbc.org/ at Stephen B. Thacker CDC Library on March 20, 2020

been shown to inhibit neoplastic transformation (23). Inhibition of AP-1 activity in transformed JB6 RT101 cells causes reversion from the tumor phenotype (24). Furthermore, a recent study, using transgenic mice, has demonstrated that AP-1 transactivation is required for tumor promotion (25). In light of the important role of AP-1 activation in neoplastic transformation and tumor promotion, we hypothesized that the silica-induced AP-1 activation may play a critical role in silica-induced carcinogenesis.

Earlier studies have suggested that FFSi exhibits increased surface reactivity compared with ASi (12, 13). Because the pulmonary response to silica differs in the chronic and acute presentation of disease, we proposed that at least part of the acute response is due to some unique characteristics of the dust inhaled. Acute silicosis is commonly associated with sandblasting, rock drilling, tunneling, and silica mill operations, *i.e.* operations in which silica particles are crushed or sheared (2, 13).

Based on the early reports that FFSi was more surface-reactive than ASi, we proposed that these surface features might be responsible for the enhanced carcinogenic effects of silica in the lung (17, 18). In the present study, the cytotoxic and biologic activities of FFSi *versus* ASi were investigated by comparing their effects on the phosphorylation of MAPKs and AP-1 activation. *In situ* generation of ROS by cells stimulated with silica was studied using fluorescence staining and ESR. Finally, the role of ROS in silica-induced AP-1 activation was evaluated.

MATERIALS AND METHODS

Reagents—SOD, *N*-acetyl-cysteine, DMPO, sodium formate, and PVPNO were purchased from Sigma Chemical Co. (St. Louis, MO). Catalase was purchased from Roche Molecular Biochemicals (Indianapolis, IN). The spin trap, DMPO, was purified by charcoal decolorization and vacuum distillation. DMPO solution, thus purified, did not contain any ESR-detectable impurities. Chelex 100 chelating resin was purchased from Bio-Rad Laboratories (Richmond, CA). The phosphate buffer (pH 7.4) was treated with Chelex 100 to remove transition metal ion contaminants. Eagle's MEM was obtained from Whittaker Biosciences (Walkersville, MD). FBS, gentamicin, and L-glutamine were purchased from Life Technologies, Inc. (Gaithersburg, MD). Luciferase assay substrate was obtained from Promega (Madison, WI). PhosphoPlus MAPK antibody kits were purchased from New England BioLabs (Beverley, MA). H_2DCFDA and dihydroethidium were obtained from Molecular Probes (Eugene, OR).

Preparation of Freshly Fractured Silica—Crystalline silica was obtained from the Generic Center, Pennsylvania State University (State College, PA). The detailed method for preparation of the FFSi has been described elsewhere (14). Briefly, crystalline silica (0.2–10 mm in diameter) was ground for 30 min using a ball grinder equipped with agate mortar and balls. The ground silica was sieved through a 10-μm mesh filter for 20 min before use. Purity was checked using x-ray diffraction spectrometry, and diameter was determined by morphometric analyses, which indicated that fractured silica had a purity of 99.5% and a mean diameter of 3.7 μm.

Cell Culture—The mouse JB6/AP/κB cell line, which was stably transfected with an AP-1 luciferase reporter plasmid (18), was cultured in Eagle's MEM containing 5% FBS, 2 mM L-glutamine, and 50 μg of gentamicin/ml.

Assay of AP-1 Activity in Vitro—A confluent monolayer of JB6/AP/κB cells was trypsinized, and 5×10^4 viable cells (suspended in 1 ml of Eagle's MEM supplemented with 5% FBS) were added to each well of a 24-well plate. Plates were incubated at 37 °C in a humidified atmosphere of 5% CO_2. Twelve hours later, cells were cultured in Eagle's MEM supplemented with 0.5% fetal bovine serum for 12–24 h to minimize basal AP-1 activity and then exposed to silica in the same medium to monitor the effects on AP-1 induction. The cells were extracted with 200 μl of 1× lysis buffer provided in the luciferase assay kit by the manufacturer. Luciferase activity was measured using a Monolight luminometer, model 3010 (18). The results were expressed as relative AP-1 activity compared with untreated controls.

Protein Kinase Phosphorylation Assay—Immunoblots for phosphorylation of ERKs and p38 kinase were carried out as described in the protocol of New England BioLabs (Beverly, MA), using phospho-specific antibodies against phosphorylated sites of ERKs and p38 kinase. Non-phospho-specific antibodies against ERKs and p38 kinase proteins provided in each assay kit were used to normalize the phosphorylation assay by using the same transferred membrane blot.

ESR Measurements—All ESR measurements were conducted using a Varian E9 ESR spectrometer and a flat cell assembly. Hyperfine couplings were measured (to 0.1 G) directly from magnetic field separation using K_3CrO_8 and 1,1-diphenyl-2-picrylhydrazyl as reference standards. An EPRDAP 2.0 program was used for data acquisition and analysis. Reactants were mixed in test tubes in a final volume of 450 μl. The reaction mixture was then transferred to a flat cell for ESR measurement. The concentrations given in the figure legends are final concentrations. All experiments were performed at room temperature and under ambient air except those specifically indicated.

H_2O_2 Measurements—JB6 cells (1×10^6) suspended in 1 ml PBS were incubated with or without silica for 30 min. H_2O_2 generation was monitored by measuring the change in fluorescence of scopoletin (0.72 mM) in the presence of horseradish peroxidase (6.6 units/ml). Fluorescence was monitored at an excitation wavelength of 350 nm and an emission wavelength of 460 nm using a Cytofluor multiwell plate reader series 4000 (PerSeptive Biosystems Inc., Framingham, MA).

H_2O_2 and O_2^- Assay in Intact Cells—Dihydroethidium and H_2DCFDA are specific dyes used for staining O_2^- and H_2O_2 produced by intact cells (26, 27). JB6 cells (2×10^4/well) were seeded onto a glass coverslip in the bottom of a well of a 24-well plate for 24 h. The cells were treated with FFSi or ASi in the presence of dihydroethidium (2 μM) or H_2DCFDA (5 μM) for 30 min. The cells were then washed in PBS and fixed with 10% buffered formalin. The glass coverslip was mounted on a microscope slide and observed under a Sarastro 2000 (Molecular Dynamics, Sunnyvale, CA) laser scanning confocal microscope fitted with an argon-ion laser.

Oxygen Consumption Measurements—Oxygen consumption measurements were carried out using a Gilson Oxygraph (Model 516, Gilson Medical Electronics, Middleton WI). Cell concentration was 6.25×10^5/ml, and measurements were made over a period of 10 min.

Statistical Analysis—Data presented are the means ± S.E. of values compared and analyzed using a one-way ANOVA. Statistical significance was determined by two-tailed Student's *t* test for paired data, and considered significant at $p \leq 0.05$.

RESULTS

Induction of AP-1 Activation by FFSi versus ASi—Earlier studies have suggested that FFSi was more surface-reactive than aged silica (12, 13). To explore the differential effects of FFSi and ASi on the induction of AP-1 activity, 5×10^4 JB6 cells were exposed for 24 h to various doses (10–300 μg/ml) of freshly fractured or fractured silica aged for 12 months. The AP-1 activation induced by FFSi was significantly higher than that of ASi in JB6 cells (Fig. 1). FFSi induced significant AP-1 activation at a concentration of 80 μg/ml silica, reaching a maximum activation at 200 μg/ml. The maximum AP-1 induction by FFSi increased 8-fold compared with controls, whereas the maximum AP-1 induction by the silica aged for 12 months increased less than 3-fold compared with controls. These results indicate that FFSi exhibited a greater effect on AP-1 induction than ASi.

Induction of AP-1 Activity by Freshly Fractured Silica and the Decay of the Induction with Time after Fracturing—To further explore the decay of AP-1 induction by silica with time after fracturing (aging), the induction of AP-1 activation by FFSi or fractured silica aged for 2 weeks, 8 weeks, 3 months, 6 months, or 12 months was monitored in the same experiment. JB6 cells (5×10^4) were exposed to 200 μg/ml silica for 24 h, and the luciferase activity was measured as described under "Material and Methods." As shown in Fig. 2, the AP-1 induction by silica was decreased with aging. Silica-induced AP-1 activation decreased by 35%, 65%, or 75% after 8 weeks, 6 months, or 12 months of storage, respectively. The half time for the decrease in the ability of fractured silica to activate AP-1 was proximately 3 months. Fractured silica still produced a 2.5-fold increase in AP-1 induction after 12 months of storage.

Phosphorylation of MAPKs Induced by FFSi and the Decline

Downloaded from http://www.jbc.org/ at Stephen B. Thacker CDC Library on March 20, 2020

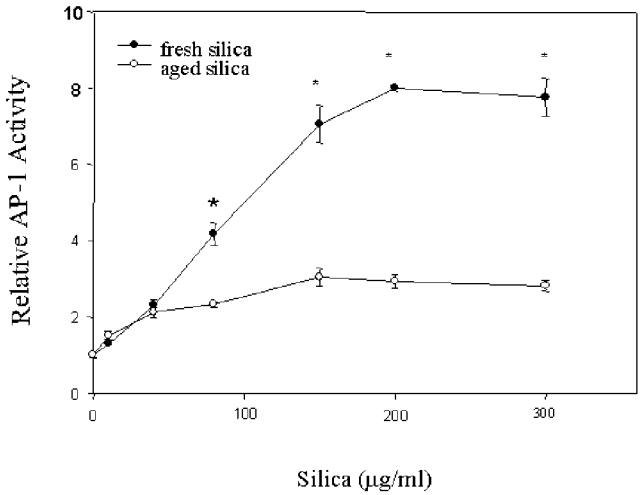

FIG. 1. **Dose-dependent induction of AP-1 activation by freshly fractured silica *versus* aged silica.** JB6 cells (5×10^4 in 1 ml of MEM medium with 5% fetal bovine serum), stably transfected with AP-1 luciferase reporter plasmid, were seeded into each well of a 24-well plate. After overnight culture at 37 °C, the cells were cultured in MEM plus 0.1% fetal bovine serum for 24 h. Then the cells were treated for 24 h with various concentrations of freshly fractured silica or fractured silica aged for 1 year. The AP-1 activity was measured by the luciferase activity assay as described under "Materials and Methods." Results, presented as relative AP-1 induction compared with the untreated control cells, are means and standard errors of eight assay wells from two independent experiments. *, a significant increase of freshly fractured silica from aged silica ($p \leq 0.05$).

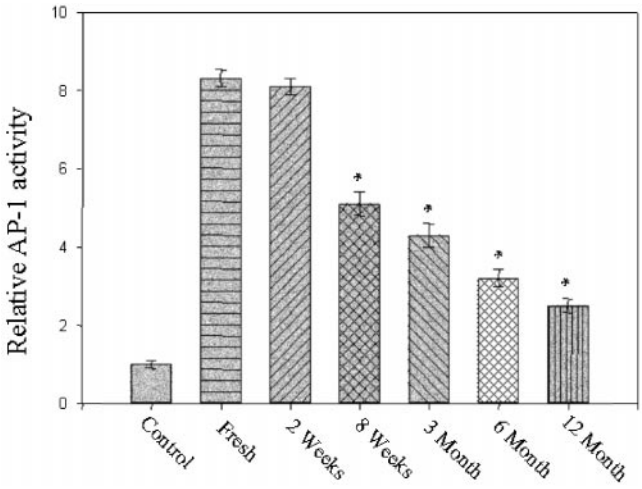

FIG. 2. **Induction of AP-1 activity by freshly fractured silica and the decay of the induction with time after fracturing.** JB6 cells (5×10^4 cells in 1 ml of MEM medium containing 5% of fetal bovine serum) were seeded into each well of a 24-well plate. After overnight culture at 37 °C, cells were cultured in the same medium plus 0.1% fetal bovine serum for 24 h. The cells were then exposed for 24 h to 200 μg/ml freshly fractured silica or silica aged for various times after fracturing. Other experimental conditions were the same as those described in the legend to Fig. 1. Results, presented as relative AP-1 induction compared with the untreated control cells, are means ± S.E. of eight assay wells from two independent experiments. *, a significant decrease from cells treated with freshly fractured silica ($p \leq 0.05$).

of Induction with Aging—Previous studies in our laboratory have indicated that silica-induced AP-1 activation is mediated through phosphorylation of MAPKs family members, ERKs and p38 kinases (18). To investigate the effects of FFSi *versus* ASi on activation of MAPKs, phosphorylation of ERKs and p38 kinases was examined. JB6 cells cultured in MEM medium in 6-well plates were exposed for 30 min to 150 μg/ml freshly fractured silica or fractured silica aged for different time periods as indicated. Then the cells were lysed by sample buffer

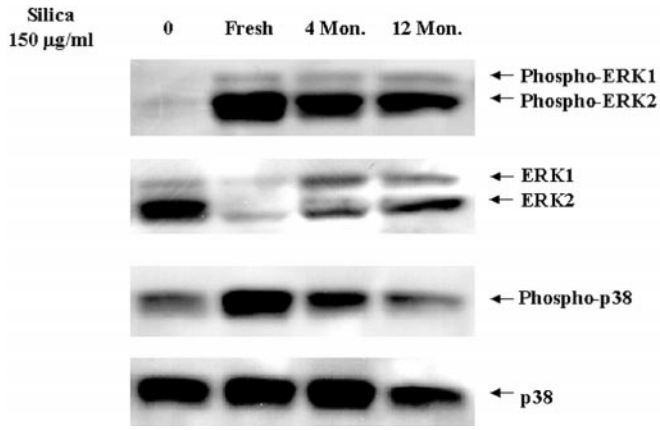

FIG. 3. **Phosphorylation of ERKs and p38 kinase induced by FFSi and the decline of induction with aging.** JB6 P^+ cells were cultured in 5% FBS MEM medium in 6-well plates until 80% confluent and then cultured in 0.1% FBS MEM medium for 24 h. Then the cells were exposed for 30 min to 150 μg/ml freshly fractured silica or fractured silica aged for different time periods as indicated. The phosphorylated and nonphosphorylated p38 kinase and ERKs proteins in the cell lysate were assayed using a PhosphoPlus MAPKs kit from New England BioLabs. The phosphorylated proteins and nonphosphorylated proteins were detected by using the same transferred membrane blot following a stripping procedure.

and the phosphorylation of ERKs or p38 kinase was analyzed as described in the protocol of New England BioLabs. Phosphorylation of ERKs or p38 kinase was greater after exposure of the cells to FFSi than ASi (Fig. 3). These results were correlated with the AP-1 activation induced by FFSi or ASi.

Effects of Antioxidant Reagents on Silica-induced AP-1 Activation and Phosphorylation of MAPKs—Because FFSi was more potent than ASi, we hypothesized that ROS may be involved in silica-induced AP-1 stimulation. To examine this hypothesis, the effects of antioxidants and other reagents on silica-induced AP-1 activation and phosphorylation of MAPKs were investigated. JB6 cells (5×10^4) cultured in 24-well plates were pretreated for 1 h with antioxidants and other reagents. Then the cells were exposed to 150 μg/ml FFSi in the presence of the same reagents for 24 h and the luciferase activity of the cell lysate was tested. The effects of antioxidants and other reagents on silica-induced AP-1 activation are shown in Fig. 4. Catalase, a H_2O_2-scavenging enzyme, strongly inhibited silica-induced AP-1 activation by 90%. Sodium formate, an $^{\cdot}OH$ radical scavenger, had no effect on the induction. SOD, a $O_2^{\cdot-}$ radical scavenger that generates H_2O_2, increased the AP-1 activation by 70%. Deferoxamine, a metal ion chelator, had a slight inhibitory effect. *N*-Acetylcysteine, a thio-containing antioxidant, or PVPNO, which binds to silanol groups on the silica surface, significantly inhibited the AP-1 induction. Similar results were obtained for the effects of these reagents on silica-induced phosphorylation of p38 kinase and ERKs. Catalase, a H_2O_2 scavenger, inhibited both p38 kinase and ERKs phosphorylation induced by silica, whereas SOD, which generates H_2O_2, enhanced the phosphorylation (Fig. 5, *A* and *B*). In contrast, formate, a $^{\cdot}OH$ scavenger, was ineffective. These results suggest that H_2O_2 might be the mediator for stimulation of p38 and ERKs signal transduction pathways leading to AP-1 induction.

ROS Generation from JB6 Cells Stimulated by Silica—To confirm that ROS are involved in silica-induced AP-1 activation, ESR spin trapping was used to detect ROS generation during cellular reactions in the presence of silica (28, 29). Freshly fractured silica or JB6 cells alone did not generate any detectable radical signal (Fig. 6, *a* and *b*). Whereas freshly ground silica plus JB6 cells generated a spin adduct signal (Fig.

Downloaded from http://www.jbc.org/ at Stephen B. Thacker CDC Library on March 20, 2020

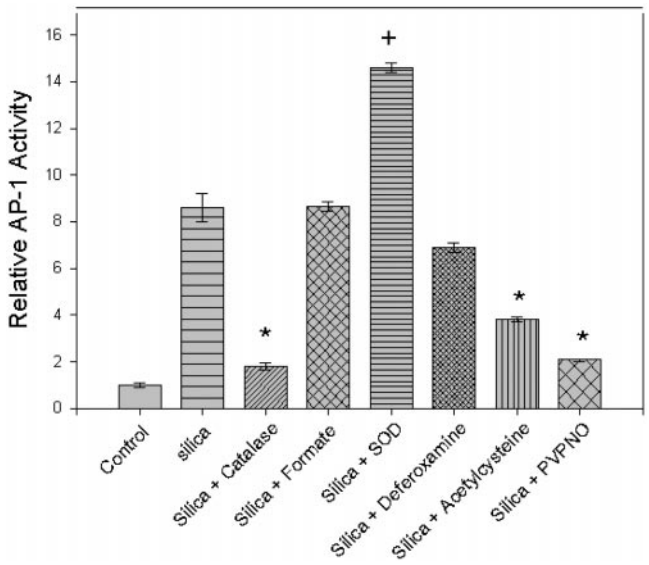

FIG. 4. **Effect of antioxidants and other reagents on silica-induced AP-1 activation.** JB6 cells were seeded into each well of a 24-well plate. After overnight culture at 37 °C, cells were incubated in the same medium plus 0.1% fetal bovine serum for 24 h. The cells were then exposed for 24 h to 150 μg/ml freshly fractured silica and various reagents as indicated. The concentrations of the reagents used were: catalase, 10,000 units/ml; sodium formate, 2 mM; SOD, 500 units/ml; deferoxamine, 1 mM; *N*-acetylcysteine, 1 mM; PVPNO, 50 μg/ml. Other experimental conditions were the same as those described in the legend to Fig. 1. Results, presented as relative AP-1 induction compared with the untreated control cells, are means ± S.E. of eight assay wells from two independent experiments. *, a significant decrease from cells treated with freshly fractured silica ($p \leq 0.05$). +, a significant increase from cells treated with freshly fractured silica ($p \leq 0.05$).

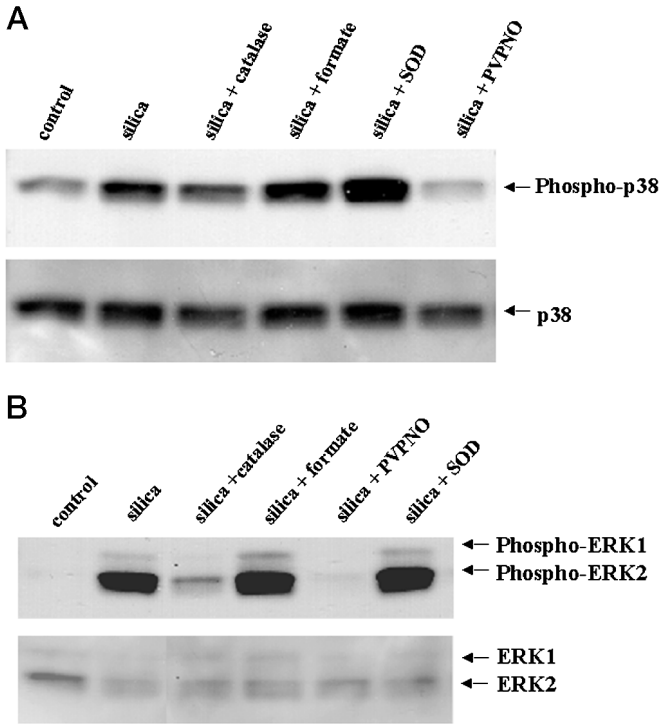

FIG. 5. **Effect of antioxidant reagents on silica-induced phosphorylation of p38 kinase and ERKs.** JB6 P^+ cells were cultured in 5% FBS MEM medium in 6-well plates until 80% confluent and then cultured in 0.1% FBS MEM medium for 24 h. The cells were then exposed to 150 μg/ml FFSi in the presence of various antioxidants or other reagents as indicated. The concentrations of the reagents used were: catalase, 10,000 units/ml; sodium formate, 2 mM; SOD, 500 units/ml; PVPNO, 50 μg/ml. The cells were lysed and phosphorylated, and nonphosphorylated p38 kinase protein (*A*) and ERKs proteins (*B*) were assayed using a PhosphoPlus MAPKs kit from New England BioLabs. The phosphorylated and nonphosphorylated proteins were analyzed by using the same transferred membrane blot following a stripping procedure.

6*c*) consisting of a 1:2:2:1 quartet with hyperfine splitting of $a_N = a_H = 14.8$ G, where a_N and a_H denote hyperfine splitting of the nitroxyl nitrogen and α-hydrogen, respectively. Based on this splitting and the 1:2:2:1 line shape, the spectrum was assigned to the DMPO-OH adduct, which is an example of $^{\bullet}OH$ radical generation. Catalase significantly decreased this signal, indicating the importance of H_2O_2 (Fig. 6*d*). Addition of SOD failed to inhibit the signal (Fig. 6*e*). Addition of H_2O_2 increased the signal intensity (Fig. 6*f*). Because DMPO-OH signal may be generated by a mechanism other than $^{\bullet}OH$ trapping (30), spin trapping competition experiments were performed for verification of $^{\bullet}OH$ generation. In these experiments the $^{\bullet}OH$ radical abstracts a hydrogen atom from formate, resulting in a decrease of DMPO-OH spin adduct signal intensity. As shown in Fig. 6*g*, addition of formate indeed reduced the signal intensity, showing that $^{\bullet}OH$ radicals were generated and trapped in the reaction system. Addition of deferoxamine, which chelates the metal ions such as Fe(II) to make them less reactive toward H_2O_2, also decreased the signal intensity (Fig. 6*h*), indicating that a metal-mediated Fenton or Fenton-like reaction plays a key role in $^{\bullet}OH$ generation from the silica-stimulated cells. Addition of *N*-acetyl-L-cysteine, a general antioxidant, decreased the adduct signal (Fig. 6*i*). Incubation of silica aged for 1 year with the cells produced only a very week signal (Fig. 6*j*).

The above results suggest that H_2O_2 might play a key role on silica-induced AP-1 and MAPK activation (Figs. 4 and 5). Next, we measured the H_2O_2 generation by JB6 cells upon stimulation with silica. JB6 cells were incubated with FSi (1 mg/ml) for 30 min, and the generation of H_2O_2 was measured as described under "Materials and Methods." As shown in Fig. 7, the generation of H_2O_2 by JB6 cells treated with FSi was markedly increased compared with untreated control cells. Catalase substantially inhibited silica-induced H_2O_2 generation by JB6 cells. In contrast, SOD had no significant effect. These results are parallel and comparable with the studies on the effect of catalase and SOD on silica-induced AP-1 and MAPK activation (Figs. 4 and 5). The data also provide more evidence for the important role of H_2O_2 on silica-induced AP-1 activation.

Detection of ROS Generation in Intact Cells—To further confirm the ROS generation by JB6 cells stimulated with silica, cells treated with silica were analyzed by intracellular staining for H_2O_2 and $O_2^{\bullet-}$. H_2DCFDA, a specific fluorescent dye for H_2O_2, and dihydroethidium, a specific fluorescent dye for $O_2^{\bullet-}$, were applied to cells to monitor ROS generation. In the presence of FFSi, the fluorescent signals of both H_2O_2 and $O_2^{\bullet-}$ were dramatically increased within 30 min after treatment of the cells (Fig. 8). In the presence of silica aged for 1 year, the signals were substantially less intense than those for the cells treated with FFSi (Fig. 8). Fluorescence was displayed using a pseudo-color intensity scale where low intensity sites appear *blue*, and increasingly high intensity areas are displayed as *green*, *yellow*, *red*, or *white*.

Increased Oxygen Consumption during the Interaction of JB6 Cells with Silica—The above results indicate that $O_2^{\bullet-}$ and H_2O_2 are generated during the interaction of JB6 cells with silica. If this is the case, exposure of the cells to silica should result in an increased rate of oxygen consumption. To test this hypothesis the rate of oxygen consumption by JB6 cells (6.25×10^5) in the presence or absence of fresh or aged silica was monitored using a Gilson Oxygraph. The results are presented in Fig. 9. Cells alone consumed molecular oxygen at a steady basal rate,

Downloaded from http://www.jbc.org/ at Stephen B. Thacker CDC Library on March 20, 2020

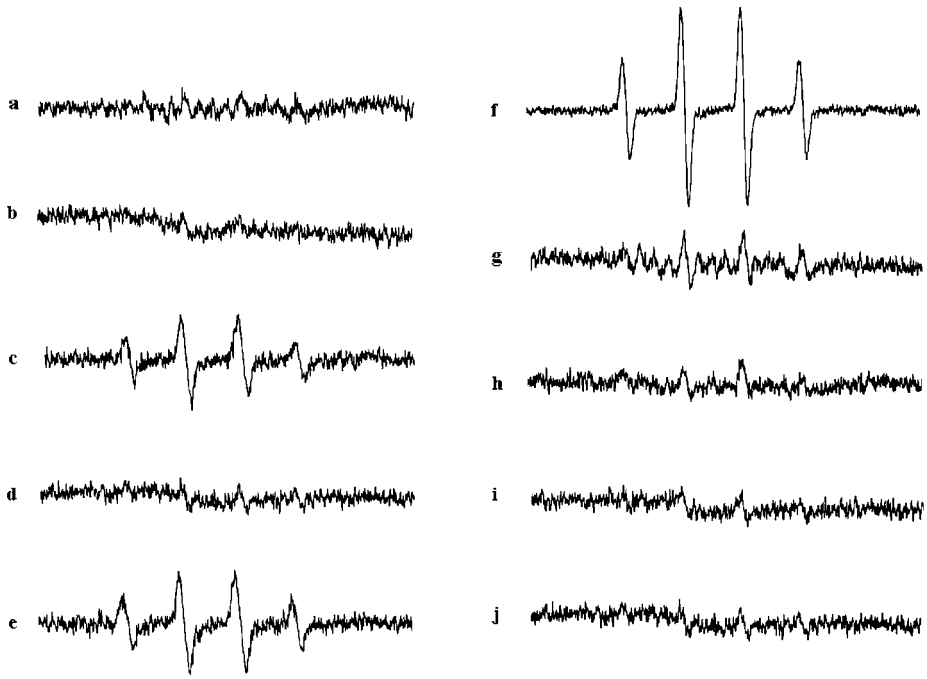

FIG. 6. **ESR signals generated by DMPO-OH adducts obtained from JB6 cells or cells treated with silica.** ESR spectra recorded for 1 min from incubation mixtures containing PBS and 100 mM DMPO: (*a*) freshly fractured silica (150 μg/ml); (*b*) JB6 cells (1×10^6); (*c*) JB6 cells (1×10^6) plus freshly fractured silica (150 μg/ml); (*d*) same as *c* but with 1000 units/ml catalase; (*e*) same as *c* but with 2000 units/ml SOD; (*f*) same as *c* but with 1 mM of H_2O_2; (*g*) same as *c* but with 50 mM sodium formate; (*h*) same as *c* but with 1 mM deferoxamine; (*i*) same as *c* but with 10 mM *N*-acetyl-L-cysteine; (*j*) JB6 cells (1×10^6) and 150 μg/ml 1-year-old silica. The spectrometer settings were: receiver gain, 2.5×10^5; time constant, 0.3 s; modulation amplitude, 1.0 G; scan time, 3 min; magnetic field, 3340 ± 100 G.

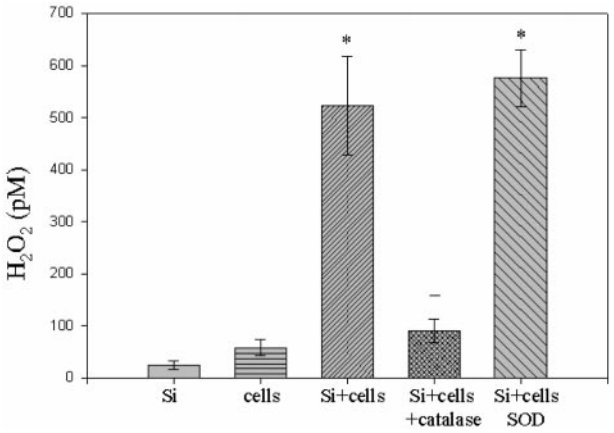

FIG. 7. **H_2O_2 generation from JB6 cells treated with silica.** JB6 cells (1×10^6) were incubated with freshly fractured silica (1 mg/ml) with or without reagents as indicated for 30 min at 37 °C. Generation of H_2O_2 by the cells was monitored as described under "Materials and Methods." The concentration of reagents used were: catalase, 2000 units/ml; SOD, 1000 units/ml. Values are means ± S.E. of three experiments. *, a significant increase from cells alone ($p \leq 0.05$). –, a significant decrease from cells plus silica ($p \leq 0.05$).

whereas in the presence of FFSi oxygen consumption increased by 33%. Dismutation of O_2^- by SOD resulted in about half the amount of O_2 consumption (data not shown). In contrast, when cells were incubated with 1-year-old ASi, the oxygen consumption was no significantly different from the basal level. In the presence of PVPNO, the oxygen consumption by the cells treated with FFSi was significantly decreased.

DISCUSSION

Crystalline silica is a recently designated carcinogen and is strongly associated with silicosis, but the molecular and cellular mechanisms involved in the silica-induced pathogenesis are not fully understood (3, 17). We hypothesize that silica-mediated free radical reactions may cause a persistent oxidative stress in the lung and play a key role in the mechanism of silica-induced carcinogenesis. Most of the studies concerning the role of ROS in silica-induced cytotoxicity have been limited to lipid peroxidation, DNA damage, and other critical changes in noncellular systems (10–14). However, our previous study has shown that silica induces AP-1 activation in cell and animal models through ERKs and p38 kinase pathways (18). In the present study, we show that ROS is the mediator for silica-induced AP-1 activation. By comparing of AP-1 activation induced by FFSi *versus* ASi, we found that AP-1 activation induced by FFSi was 4-fold higher than that of silica fractured and aged for 1 year. The enhanced potency of FFSi was also exhibited for silica-induced phosphorylation of ERKs and p38 kinase. We also demonstrate that H_2O_2, formed during the interaction of silica with the cells, might be a reactive intermediate responsible for silica-induced AP-1 activation and phosphorylation of MAPKs.

The results from the present study show that silica-induced AP-1 activation involves ROS-mediated reactions. A major role of H_2O_2 in silica-induced AP-1 activation is supported by the following observations: (*a*) catalase, whose function is to remove H_2O_2, blocked the AP-1 activation and phosphorylation of MAPKs; (*b*) SOD, which converts O_2^- to H_2O_2, enhanced AP-1 activation; (*c*) sodium formate, a scavenger of $^{\bullet}OH$ radical, did not exhibit any effect; and (*d*) treatment of cells with freshly fractured silica resulted in a 9.5-fold increase in H_2O_2 production. As for ROS generation, it may be noted that our earlier studies (12–15) have shown that FFSi generates silicon-based radicals ($Si^{\bullet}$, $SiO^{\bullet}$, and $SiOO^{\bullet}$). These silicon radicals can generate ROS upon reaction with aqueous medium. The present study shows that silica is also able to generate ROS via stimulation of cells and that this ROS production occurs at a lower concentration of silica than in noncellular systems. During these processes, molecular oxygen was consumed to generate O_2^- radical, which produced H_2O_2 by dismutation. H_2O_2 generated the $^{\bullet}OH$ radical via a Fenton or Fenton-like reaction. The following experimental observations support the above pathway of ROS generation from silica-stimulated cells: (*a*) Oxygen consumption assay showed that silica-stimulated cells consumed molecular oxygen; (*b*) both O_2^- and H_2O_2 were generated as measured by fluorescence staining of silica-exposed cells; (*c*) ESR spin trapping studies showed that $^{\bullet}OH$ radicals were generated; (*d*) catalase inhibited the signal, whereas H_2O_2 enhanced it; (*e*) addition of SOD, whose function is to remove $O_2^{\bullet -}$, did not substantially alter $^{\bullet}OH$ generation; and (*f*) addition

Downloaded from http://www.jbc.org/ at Stephen B. Thacker CDC Library on March 20, 2020

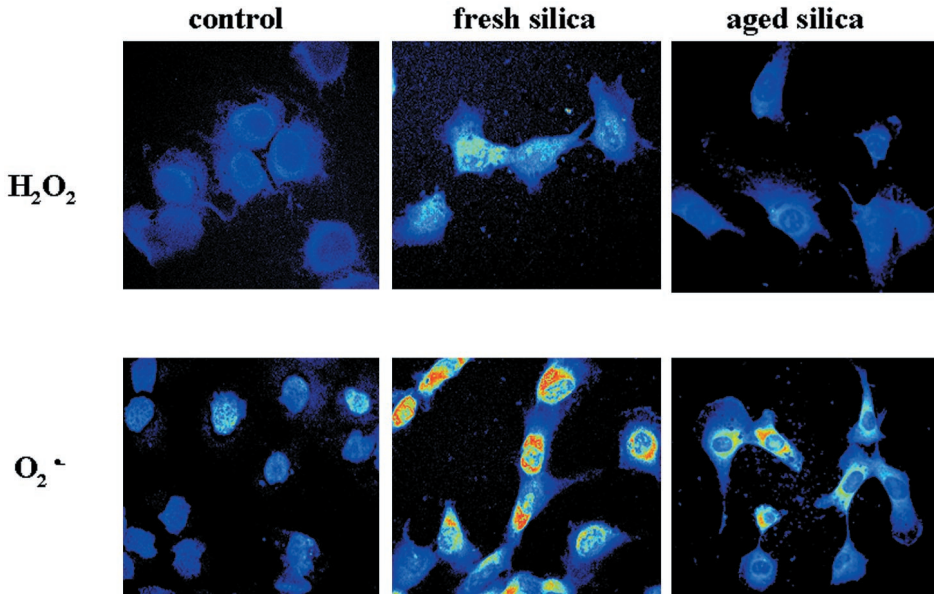

FIG. 8. **Confocal micrograph of $O_2^{\cdot-}$ and H_2O_2 generation in intact cells treated with silica.** JB6 cells were treated with 150 μg/ml FFSi in the presence of 2 μM dihydroethidium or 5 μM H_2DCFDA for 30 min. The cells were washed once with PBS and fixed with 10% buffered formalin. The images were captured with a laser scanning confocal microscope. The *bright greenish yellow areas* in the cells represent oxidized DCFH-DA, and the *bright reddish orange spots* represent oxidized dihydroethidium showing the intracellular localization of H_2O_2 and $O_2^{\cdot-}$, respectively.

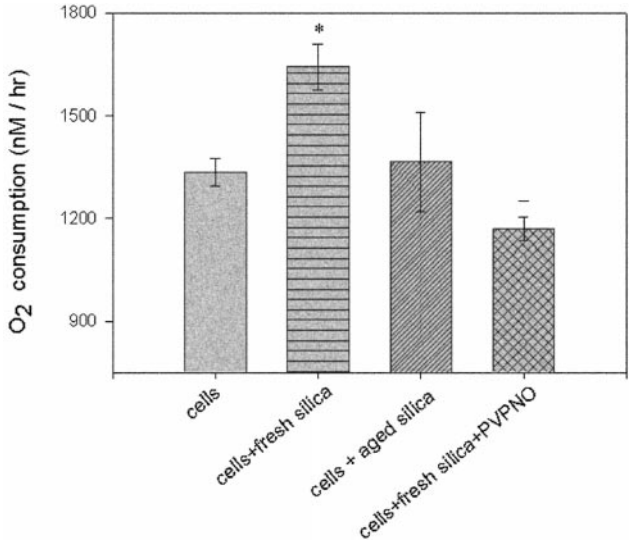

FIG. 9. **Oxygen consumption of JB6 cells.** Oxygen consumption by JB6 cells (6.25×10^5) in PBS with or without silica. *Bar 1*, cells in PBS; *bar 2*, cells treated with 150 μg/ml freshly fractured silica; *bar 3*, cells treated with 150 μg/ml fractured silica aged for 1 year; *bar 4*, cells treated with freshly fractured silica (150 μg/ml) in the presence of PVPNO (50 μg/ml). *Each bar* indicates the mean ± S.E. of three experiments. *, a significant increase from control ($p \leq 0.05$). –, a significant decrease from FFSi ($p \leq 0.05$).

of deferoxamine, which chelates metal ions such as Fe(II) to make them less reactive toward H_2O_2, reduced $^{\cdot}OH$ generation.

The signal transduction pathways leading to AP-1 activation and the possible involvement of ROS were also investigated in the present study. It is well known that stress-related signals, such as UV radiation or ROS, induce the activation of MAPK pathways. ERKs, JNKs, and p38 are important signal transduction pathways involved in AP-1 activation, and AP-1 is one of the downstream targets of these three MAPK members. An earlier study has shown that FFSi caused phosphorylation of ERKs and p38, but not JNKs (18). The results obtained from the present study show that FFSi caused phosphorylation of both p38 and MAPKs to a greater degree than that induced by ASi. Moreover, catalase inhibited the silica-induced phosphorylation of ERKs and p38 kinase, suggesting that H_2O_2 is required in the phosphorylation process. These results further suggest that H_2O_2 plays a key role in AP-1 activation.

It should be noted that PVPNO significantly inhibited silica-induced AP-1 activation and phosphorylation of MAPKs. SiOH groups on the silica surface have been proposed to be involved in silica-induced cellular damage. Chemical modification of the silica surface can be used to reduce toxicity *in vitro* and fibrosis *in vivo* (31). It is known that when silica particles are exposed to water, surface silicon-oxygen bonds (Si–O) are hydrated, resulting in the formation of SiOH groups. PVPNO is able to bind to SiOH groups. It has been reported that PVPNO inhibits silica-induced toxicity and decreases or delays the development of silicosis in experimental animals and humans. It also blocks the interaction of the silica surface with phosphate groups of DNA *in vitro*. It has been reported that PVPNO inhibits silica-induced ROS generation in cells (31, 32).

The present study used mouse epidermal cells as an *in vitro* model system. These epidermal cells were employed, because they exhibit a stronger although qualitatively similar response compared with bronchial epithelial cells (18). Furthermore, in our previous studies, we have shown that *in vivo* responses in transgenic mice were qualitatively similar to studies in epidermal cells (18).

Our studies show that FFSi particles are much more potent in inducing AP-1 activation than are ASi. Upon stimulation by silica, JB6 cells are able to generate a whole spectrum of ROS. Compared with a direct reaction between silica with aqueous medium, the yield of ROS generation from silica-stimulated cells is much higher. Among the ROS produced, H_2O_2 appears to be the species responsible for silica-induced AP-1 activation. Our novel findings suggest that ROS may play a key role in silica-induced oncogene stimulation. Because oncogene stimulation is thought to be involved in carcinogenesis, there is a need to study further the mechanisms involved in this process.

REFERENCES

1. Reiser, K. M., and Last, J. A. (1979) *Toxicology* **13,** 51–72
2. Craighead, J. S., Kleinerman, J., Abraham, J. L., Gibbs, A. R., Green, F. H. Y., Harley, R. A., Ruettner, J. R., Vallyathan, N. V., and Juliano E. B. (1988) *Arch. Pathol. Lab. Med.* **112,** 673–720
3. McDonald, J. C. (1996) in *Silica and Silica-Induced Lung Diseases* (Castranova V., ed) pp. 383–406, CRC Press, Boca Raton, FL
4. International Agency for Research on Cancer (1987) *IARC Monogr. Eval. Carcinog. Risks Chem. Hum.* **42,** 1–239
5. Saffiotti, U., Williams, A. O., Daniel L. N., Kaighn, M. E., Mao, Y., and Shi, X. (1996) in *Silica and Silica-Induced Lung Diseases* (Castranova V., ed) pp. 345–381, CRC Press, Boca Raton, FL
6. Saffiotti, U. (1992) *Prog. Clin. Biol. Res.* **374,** 51–69
7. Simonato, L., and Saracci, R. (1990) *IARC. Sci. Publ.* **97,** 1–5
8. Wagner, M. M. F. and Wagner, J. C. (1972) *J. Natl. Cancer Inst.* **49,** 81–91
9. International Agency for Research on Cancer (1997) *IARC Monogr. Eval.*

Downloaded from http://www.jbc.org/ at Stephen B. Thacker CDC Library on March 20, 2020

Carcinog. Risks Hum. **68,** 1–475
10. Shi, X., Mao, Y., Daniel, L. N., Saffiotti, U., Dalal, N. S., and Vallyathan, V. (1994) *Environ. Health Perspect.* **102,** Suppl. 10, 149–154
11. Daniel, L. N., Mao, Y., Williams, A. O., and Saffiotti, U. (1995) *Scand. J. Work. Environ. Health* **21,** Suppl. 2, 22–26
12. Shi, X., Dalal, N. S., and Vallyathan, V. (1988) *J. Toxicol. Environ. Health* **25,** 237–245
13. Vallyathan, V., Shi, X. L., Dalal, N. S., Irr, W., and Castranova, V. (1988) *Am. Rev. Respir. Dis.* **138,** 1213–1219
14. Dalal, N. S., Shi, X., and Vallyathan, V. (1990) *J. Toxicol. Environ. Health* **29,** 307–316
15. Dalal, N. S., Shi, X., and Vallyathan, V. (1990) *Free Radic. Res. Commun.* **9,** 259–266
16. Chen, F., Lu, Y., Demers, L. M., Rojanasakul, Y., Shi, X., Vallyathan, V., and Castranova, V. (1998) *Ann. Clin. Lab. Sci.* **28,** 1–13
17. Shi, X., Castranova, V., Halliwell, B., and Vallyathan, V. (1998) *J. Toxicol. Environ. Health B. Crit. Rev.* **1,** 181–197
18. Ding, M., Shi, X., Dong, Z., Chen, F., Lu, Y., Castranova, V., and Vallyathan, V. (1999) *J. Biol. Chem.* **274,** 30611–30616
19. Angel, P., and Karin, M. (1991) *Biochim. Biophys. Acta* **1072,** 129–157
20. Bernstein, L. R., and Colburn, N. H. (1989) *Science* **244,** 566–569
21. Barthelman, M., Chen, W., Gensler, H. L., Huang, C., Dong, Z., and Bowden, G. T. (1998) *Cancer Res.* **58,** 711–716
22. Crawford, H. C., and Matrisian, L. M. (1996) *Enzyme Protein* **49,** 20–37
23. Huang, C., Ma, W., Bowden, G. T., and Dong, Z. (1996) *J. Biol. Chem.* **271,** 31262–31268
24. Dong, Z., Lavrovsky, V., and Colburn, N. H. (1995) *Carcinogenesis* **16,** 749–756
25. Young, M. R., Li, J. J., Rincon, M., Flavell, R. A., Sathyanarayana, B. K., Hunziker, R., and Colburn, N. (1999) *Proc. Natl. Acad. Sci. U. S. A.* **96,** 9827–9832
26. Zamzami, N., Marchetti, P., Castedo, M., Zanin, C., Vayssiere, J. L., Petit, P. X., and Kroemer, G. (1995) *J. Exp. Med.* **181,** 1661–1672
27. Zamzami, N., Marchetti, P., Castedo, M., Decaudin, D., Macho, A., Hirsch, T., Susin, S. A., Petit, P. X., Mignotte, B., and Kroemer, G. (1995) *J. Exp. Med.* **182,** 367–377
28. Rosen, G. M., and Finkelstin, E. (1985) *Adv. Free Radic. Biol. Med.* **1,** 345–375
29. Britigan, B. E., Rosen, G. M., Thompson, B. Y., Chai, Y., and Cohen, M. S. (1986) *J. Biol. Chem.* **261,** 17026–17032
30. Keisuke, M., Akifumi, H., Hiroshi, I., Akira, M., and Masatoshi, N. (1992) *Can. J. Chem.* **70,** 2818–2827
31. Vallyathan, V., Mega, J. F., Shi, X., and Dalal, N. S. (1992) *Am. J. Respir. Cell Mol. Biol.* **6,** 404–413
32. Castranova, V. (1996) in *Silica and Silica-Induced Lung Diseases* (Castranova V., ed) pp. 293–298, CRC Press, Boca Raton, FL

Downloaded from http://www.jbc.org/ at Stephen B. Thacker CDC Library on March 20, 2020

Induction of Activator Protein-1 through Reactive Oxygen Species by Crystalline Silica in JB6 Cells

Min Ding, Xianglin Shi, YongJu Lu, Chuanshu Huang, Stephen Leonard, Jenny Roberts, Jim Antonini, Vince Castranova and Val Vallyathan

J. Biol. Chem. 2001, 276:9108-9114.
doi: 10.1074/jbc.M007666200 originally published online November 28, 2000

Access the most updated version of this article at doi: 10.1074/jbc.M007666200

Alerts:
- When this article is cited
- When a correction for this article is posted

Click here to choose from all of JBC's e-mail alerts

This article cites 29 references, 9 of which can be accessed free at
http://www.jbc.org/content/276/12/9108.full.html#ref-list-1

Downloaded from http://www.jbc.org/ at Stephen B. Thacker CDC Library on March 20, 2020